Report no. changed (Mar 2006): SM-316-UU

SACLANTCEN MEMORANDUM
serial no.: SM-316

SACLANT UNDERSEA RESEARCH CENTRE MEMORANDUM

A PLANE-WAVE DECOMPOSITION METHOD FOR MODELING SCATTERING FROM OBJECTS AND BATHYMETRY IN A WAVEGUIDE

J.A. Fawcett

November 1996

Report no. changed (Mar 2006): SM-316-UU

SACLANT Undersea Research Centre
Viale San Bartolomeo 400
19138 San Bartolomeo (SP), Italy

tel: +39-187-540.111
fax: +39-187-524.600

e-mail: library@saclantc.nato.int

NORTH ATLANTIC TREATY ORGANIZATION

SACLANTCEN SM-316

A plane-wave decomposition method for modeling scattering from objects and bathymetry in a waveguide

John A. Fawcett

The content of this document pertains to work performed under Project 033-3 of the SACLANTCEN Programme of Work. The document has been approved for release by The Director, SACLANTCEN.

Jan L. Spoelstra
Director

intentionally blank page

A plane-wave decomposition method for modeling scattering from objects and bathymetry in a waveguide

John A. Fawcett

Executive Summary: A better understanding of how energy is scattered in the ocean will lead to a significant improvement in our ability to detect and classify scattering objects such as mines. The energy incident upon and scattered from an object will also interact with the sea surface and sea bottom and hence, it is important to include the effects of the oceanic boundaries in the scattering model. This memorandum describes a computational approach which allows the scattering characteristics of surfaces and objects to be computed independently and then combined in a straightforward fashion to yield the scattered pressure for a given source/receiver geometry. This method provides a flexible, modular approach to solving scattering problems in oceanic waveguides. The numerical examples presented are for a scattering object located in the water, but the theory can be easily modified for the case of, for example, a buried mine.

This memorandum describes the theory and computer implementation of an object/surface scattering model. Computational results of low frequency scattering from a cylinder are presented. The cases of the cylinder in a waveguide with a flat and with a sloping bottom are considered. For some of the examples, it is also possible to compute the solutions using other, standard techniques. In these cases, the agreement between the method of this memorandum and the other methods is excellent, thus validating our technique. In the future, we hope to utilize the concepts of this paper to investigate other scattering problems of interest such as scattering from a buried cylinder below a rough interface.

intentionally blank page

A plane-wave decomposition method for modeling scattering from objects and bathymetry in a waveguide

John A. Fawcett

Abstract: In this paper a straightforward plane-wave decomposition method which can be used for solving object and/or interface scattering problems in a waveguide is described. The method utilizes the free-space scattering matrix of an object in conjunction with the medium's interface and layer matrices in order to solve the waveguide scattering problem.

Contents

A plane-wave decomposition method for modeling scattering from objects and bathymetry in a waveguide

John A. Fawcett
SACLANT Undersea Research Centre, Viale San Bartolomeo 400, 19138 La Spezia (SP), Italy

(Received 17 April 1995; accepted for publication 24 March 1996)

In this paper a straightforward plane-wave decomposition method which can be used for solving object and/or interface scattering problems in a waveguide is described. The method utilizes the free-space scattering matrix of an object in conjunction with the medium's interface and layer matrices in order to solve the waveguide scattering problem. © *1996 Acoustical Society of America.*

PACS numbers: 43.30.Dr, 43.30.Gv, 43.20.Mv [JHM]

INTRODUCTION

There has been much interest over the last several years in modeling the wave field scattered by compact objects and/or bathymetry in a geoacoustic waveguide. The approaches to this problem have been many and varied. One approach, which is appropriate for both bathymetric and object scattering problems, is to use boundary integral equation methods (BIEM)[1–2] with the waveguide's Green's function. Using this Green's function rather than, for example, a free-space Green's function means that the integral equation(s) for the unknown field quantities can be reduced to just the surface of the scattering object or a compact area of nonflat bathymetry. The disadvantage of this approach is that for general stratified, elastic media the computation of the required Green's function for the kernel of the integral equation(s) can become quite time consuming.

Other authors have considered the scattering problem for objects in a waveguide as essentially a free-space problem and have then modified the T-matrix technique to account for the wave field interactions with the waveguide boundaries.[3–5] Besides integral equation methods of solution, finite difference,[6] finite element,[7] and coupled mode[8] methods can be employed to solve waveguide scattering problems. The first two methods have the advantage that they can handle very general range-dependent problems; they have the disadvantage that the numerical grids become very large for many problems of interest. Coupled mode methods are a promising approach to waveguide scattering problems. However, when the waveguide is deep or the frequency high, the required number of modes and the amount of computation for this method becomes large. Recently, though, Knobles[9] has proposed a technique which may partially alleviate this problem.

In Ref. 10 a matched asymptotic solution method is presented which uses a parabolic equation method to describe the incident and scattered fields in the region away from the scatterer. An inner asymptotic solution is computed near the scatterer. Other techniques of solution have been discussed (e.g., Refs. 11 and 12) in which the incident field and the scattered field away from the scatterer is taken to be modal in nature but free-space T-matrix techniques are used to compute the scattered field close to the object. Parabolic equation methods which internally model the effects of scattering have also been implemented (e.g., Ref. 13).

In this paper we discuss a method which is based upon the work of Kennett,[14] Kohketsu,[15] and Kennett *et al.*[16] on generalized reflection operators for laterally varying media. Frazer and McCoy[17] have utilized the concepts of invariant embedding to model laterally varying media using pseudodifferential operators. Our approach is also similar in spirit to that of Schuster and Smith.[18] The exact T-matrix work of Refs. 3–5 also uses the idea of reflection and transition matrices in order to incorporate the effects of surrounding boundaries. Thus it is also related to the present work. We feel that the power of the approach outlined in this paper lies in its modular, flexible approach to possibly complicated scattering problems. Objects and interfaces are characterized by scattering matrices which are determined individually and by any means which the user feels is appropriate. Using the methodology outlined in this paper, it is then possible to combine these matrices in a straightforward fashion to compute the overall waveguide/object scattering response. The accurate determination of the individual scattering matrices may be nontrivial and is, of course, fundamental to the accuracy of the overall waveguide scattering problem. However, the formulae described in Sec. I for the combination of these matrices do not depend upon the methods used for their computation.

In the numerical examples at the end of the paper, we use the methodology of this paper to compute the pressure field scattered by a cylinder in a waveguide. We then give an example of the flexibility of the method by using the method's formalism to approximately solve wave propagation in a wedge-shaped (the ASA benchmark wedge[19]) waveguide. Finally, combining the scattering matrices for the wedge-shaped waveguide and the cylinder, it is straightforward to compute the scattering from a cylinder in a wedge-shaped waveguide. These particular examples were chosen because the scattering matrices for the cylinder and for the wedge waveguide can be determined semianalytically. However, it is important to note that the same methodology used in these examples can be applied to any object(s) and/or interface(s) for which the scattering matrix can be determined analytically, numerically (perhaps by using BIEM or T-matrix methods), by approximations (e.g., Kirchoff[20] small-slope

approximation[21]), by direct measurements or by any other means. The problems solved in the numerical examples, although interesting in themselves, are meant only as a simple illustration of the method's applicability.

I. THEORY

The approach we take in this paper is motivated by the fact that in a stratified waveguide the acoustic or elastic fields in homogeneous layers are naturally and simply described in terms of up- and downgoing plane waves. If we allow some layers to contain objects or nonflat interfaces, then the fields within these layers may no longer be simply described in terms of up- and downgoing waves. However, if the vertical extent to the layer is larger than the extent of the object itself, then at the bottom and top of the layer the field can be simply split into up- and downgoing plane-wave components. Thus this layer can still be characterized in terms of the object scattering of an incident plane-wave (from above or below) into up- and downgoing components. In such a manner, a fairly general waveguide can be characterized by scattering operators describing the layering of the medium, objects, and nonflat interfaces. The approach we take for building up the overall waveguide scattering solution follows the invariant embedding approach used by Kennett[22] in his work on propagation in stratified media. This is a method by which one recursively builds up the plane-wave scattering response of a composite medium. For example, suppose we have computed the response of a half-space (perhaps, layered) to downgoing incident plane waves. We now ask: what is the response of a medium consisting of the half-space with an additional object above it? We can build up the new scattering solution in terms of object and object/half-space interactions. For a downward incident wave, the object, in general, scatters a continuum of upgoing waves. It also scatters a continuum of downgoing waves, which then interact with the lower half-space. However, the response of the half-space to these waves is already known. Some energy is then reflected back toward object where it interacts and is rescattered into upgoing and downgoing components. Thus there is a sequence of object/half-space interactions, all of which can be computed in terms of the object's scattering operator and the half-space scattering operator which is assumed to have been computed. In practice, it may be that only a few of the multiple interactions are needed for the accurate computation of the new system scattering operator. However, as is discussed below, we can, in fact, analytically sum this operator series. Once the new scattering operator has been computed for incident plane waves, one can add a new object, interface, etc., to the problem and repeat the process, recursively computing the waveguide plane-wave response.

Let us now consider a waveguide with an upper interface at $z=z_A$ and a lower interface at $z=z_B$ (see Fig. 1). For simplicity, we take the medium to be homogeneous with sound speed c and unit density. A scattering object is located within the waveguide and the origin of the coordinate system is taken within the object. Conceptually, it is easiest to consider the waveguide divided into three layers; a layer above the scatterer, a layer containing the scattering object and a layer below. Within these layers, the wave fields consist of up- and downgoing waves. For example, in the upper layer we can write for the upgoing wave field,

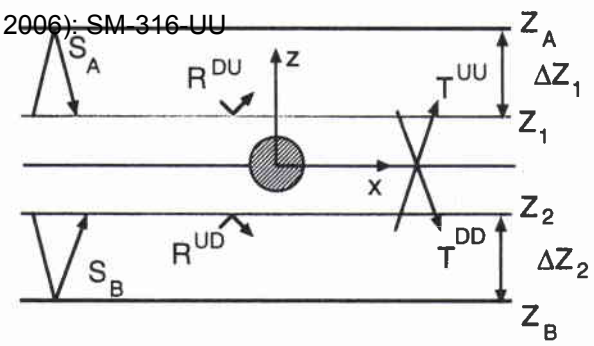

FIG. 1. Schematic drawing of a simple waveguide with a scattering object.

$$p_+ = \int_C e^{ikx \sin\phi} e^{ikz \cos\phi} a_+(\phi) d\phi \tag{1}$$

and for the downgoing wave field,

$$p_- = \int_C e^{ikx \sin\phi} e^{-ikz \cos\phi} a_-(\phi) d\phi, \tag{2}$$

where a_+ and a_- are the coefficients of the up- and downgoing plane-wave components. In these equations $k \equiv \omega/c$, ϕ represents an angle of incidence measured off the vertical axis [mathematically, $\phi \equiv \tan^{-1}(k_x/|k_z|)$ where k_x, k_z are the horizontal and vertical wave numbers of the plane-wave components] and C is a possible contour in the complex-k plane which can be used for the plane-wave representation of the Hankel function (see Fig. 2 for a schematic of a possible contour). Another possible parametrization of the integrals of Eqs. (1) and (2) would be in terms of $k_x \equiv k \sin\phi$.

We now follow the work of Kennett for stratified media[22] and previously mentioned authors[14–16] for laterally inhomogeneous media. At the top surface of the waveguide, $z=z_A$, the up- and downgoing waves are related by the generalized scattering operator S_A. The phase advancement of

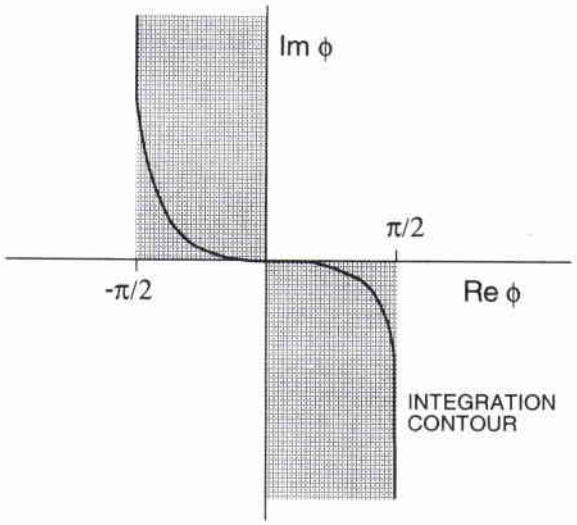

FIG. 2. Complex ϕ plane with a possible integration contour.

the wave components from z_1 to z_A and back again are also included in this operator. We use the notation that the superscript + refers to an upward propagating wave and the superscript −, a downward propagating wave. For a flat pressure release surface, this operator is diagonal (due to the fact that the interface is flat) and has entries $-\exp(2ik\cos\phi\Delta z_1)$. We define an operator R^{du} which expresses the reflection of waves incident upon the scatterer from above with reference to $z=z_1$, and an operator T^{dd} which expresses the transmission of waves from $z=z_1$ to $z=z_2$; similarly there are the operators R^{ud} and T^{uu} for the wave field in the bottom layer incident upon the object. There is also a scattering operator for the bottom boundary, S_B. For a flat surface this is a diagonal operator with elements $R(\phi)\exp(2ik\cos\phi\Delta z_2)$, where $R(\phi)$ is the reflection coefficient for the interface.

For simplicity, let us first consider the case of no upper boundary and consider the amplitudes of the plane-wave components of the incident field to be specified by the functions $\mathbf{p}_+(\phi)$ and $\mathbf{p}_-(\phi)$, respectively. We have used vector notation here, because we will later consider a discrete set of angular values. In this case, functions of angle will become vectors and operators, matrices. In the following analysis we will consider the source to be above the scatterer and the receiver above the source. Using the logic outlined below, it is straightforward to derive the operator expressions for the other possible source/scatterer/receiver geometries. The coefficients of the wave numbers (all upgoing for the layer above the source) in the upper layer is given by

$$\mathbf{p}_u(\phi)=\mathbf{p}_+(\phi)+Q\mathbf{p}_-(\phi). \tag{3}$$

The operator Q accounts for the scattering of the downward incident field by the object and the interactions of the scatterer and the bottom boundary. Writing these interactions out in systematic order, it can be seen that the operator Q is given by

$$Q=R^{du}+T^{uu}S_BT^{dd}+T^{uu}S_BR^{ud}S_BT^{dd}+T^{uu}(S_BR^{ud})^2S_BT^{dd}+\cdots \tag{4a}$$

or

$$Q=R^{du}+T^{uu}(I-S_BR^{ud})^{-1}S_BT^{dd}. \tag{4b}$$

In order to derive Eq. (4b) we have used the operator identity

$$I+X+X^2+X^3+\cdots=(I-X)^{-1}. \tag{5}$$

We have derived the above expressions assuming an infinite lower half-space. However, the lower interface operator S_B can easily be the reflection operator for a lower half-space with layers. In this case, the computation of S_B can be done using an approach similar to that described above; the overall scattering operator for the composite half-space is constructed recursively from the scattering operators of the underlying layers.

We now introduce an upper surface to the waveguide. We write

$$\mathbf{p}_u=\mathbf{p}_++Q_2(\mathbf{p}_-+S_A\mathbf{p}_+) \tag{6a}$$

and

$$\mathbf{p}_d=S_A\mathbf{p}_++S_AQ_2(\mathbf{p}_-+S_A\mathbf{p}_+). \tag{6b}$$

For the receiver below the source, we can write

$$\mathbf{p}_u=Q_2(\mathbf{p}_-+S_A\mathbf{p}_+) \tag{6c}$$

and

$$\mathbf{p}_d=\mathbf{p}_-+S_A\mathbf{p}_++S_AQ_2(\mathbf{p}_-+S_A\mathbf{p}_+). \tag{6d}$$

The quantity $\mathbf{p}_-+S_A\mathbf{p}_+$ is the effective field incident upon the scattering region from above. The operator Q_2 relates the upgoing energy from the scatterer to the initial downgoing energy and is the result of multiple interactions between the operator Q and the top surface operator S_A,

$$Q_2=Q+QS_AQ+(QS_A)^2Q+\cdots=(I-QS_A)^{-1}Q. \tag{7}$$

The downgoing components of Eq. (6b) are simply related to the upgoing components of Eq. (6a) by an additional surface reflection. The expressions of Eqs. (6c) and (6d) differ from those of Eqs. (6a) and (6b) only by the expression for the incident field.

For a source above the scatterer and the region below the scatterer we can derive the relations

$$\mathbf{p}_d^B=T^{dd}\mathbf{p}_d^U \tag{8a}$$

and

$$\mathbf{p}_u^B=(I-S_BR^{ud})^{-1}S_B\mathbf{p}_d^B, \tag{8b}$$

where the superscript B denotes below the scattering region and U refers to the upper region components determined by Eq. (6).

Once the functions $\mathbf{p}_u$ and $\mathbf{p}_d$ (either above or below scattering region) have been computed with respect to some horizontal line (usually, $z=0$) then the pressure field can be computed at a receiver location (x_r,z_r) using the formula

$$p(x_r,z_r)=\int_C e^{ikx_r\sin\phi}e^{ikz_r\cos\phi}\mathbf{p}_u(\phi)d\phi+\int_C e^{ikx_r\sin\phi}e^{-ikz_r\cos\phi}\mathbf{p}_d(\phi)d\phi. \tag{9}$$

For points which are not above or below the vertical extent of the scatterer, the simple up and downgoing plane-wave representation may not be valid. If it is desired to compute the field within the vertical extent of the scatterer, then it may be necessary to use another representation of the scattered field. This representation will likely be dependent upon the actual method used to solve the individual scattering problem. For example, a simple BIEM may be used to determine the scattering matrices for an object in a homogeneous free-space. The plane-wave representation method of this paper then gives the effective (i.e., including all the boundary interaction effects) incident plane-wave components on the scatterer; the boundary integral relations at the scatterer can then be used to generate the scattered pressure field within the section of the waveguide surrounding it (either just within the vertical extent of the scatterer or in an entire homogeneous section of the waveguide).

In practice, the operators described above become finite matrices, the integrals become finite sums, and the functionals $\mathbf{p}_+$, etc. become vectors when a discrete set of angles (some may be complex) is considered. The derivation of Eqs.

(4)–(7) provide the basic framework for combining the various object/interface scattering matrices. As mentioned in the introduction, the individual matrices S_A, S_B, R^{ud}, R^{du}, etc., can be determined by a variety of methods. If the interfaces of the waveguide are flat then S_A and S_B are diagonal with the values of the reflection coefficients for the discrete set of angles. Thus it is straightforward to include the effects of acoustic or elastic interfaces. If the interfaces are range-dependent then the scattering matrices are, in general, full and may be determined either numerically (e.g., BIEM) or by some approximation (e.g., small slope approximation[21]). The object scattering matrices may also be determined in a variety of ways. As we will consider a cylinder in the numerical examples, we outline the semianalytical computation of the scattering matrices for this case.

First, we consider the origin to be located at the center of the cylinder; then a plane wave with angle of incidence θ can be expressed in the form[23]

$$e^{ikr\cos(\beta-\theta)}=\sum_{n=-\infty}^{\infty} i^n J_n(kr)e^{in\beta}e^{-in\theta}, \tag{10}$$

where r and β are the polar coordinates with respect to the cylinder center. For a pressure release cylinder, the scattered field from the cylinder is then given by

$$p^{sc}(r,\beta)\approx-\sum_{n=-N}^{N} i^n H_n^1(kr)\alpha_n e^{in\beta}e^{-in\theta}, \tag{11}$$

where

$$\alpha_n=\frac{J_n(ka)}{H_n^1(ka)} \tag{12}$$

and a is the radius of the cylinder. Other types of cylinders are easily considered by changing the expression for α_n.

We now wish to express the scattered field in terms of plane-wave components. In order to do this, we replace $H_n^1(kr)e^{in\beta}$ in Eq. (11) by its plane-wave expansion,[23]

$$H_n^1(kr)e^{in\beta}=\frac{e^{-in\pi/2}}{\pi}\int_C e^{ikr\cos(\phi-\beta)}e^{in\phi}\,d\phi. \tag{13}$$

In fact, we use a discrete version of Eq. (13)

$$H_n^1(kr)e^{in\beta}\approx\frac{e^{-in\pi/2}}{\pi}\sum_{m=1}^{M} e^{ikr\cos(\phi_m-\beta)}e^{in\phi_m}\delta_m. \tag{14}$$

In this discretization of the integral of Eq. (13), M panels have been used with weightings δ_m. We will consider the angle of incidence $\theta=\phi_k$ to be from the same set of discrete angles as used in Eq. (14). Then we have from Eq. (11)

$$p^{sc}(r,\beta)=-\sum_{n=-N}^{N} i^n\alpha_n\frac{e^{-in\pi/2}}{\pi}\times\sum_{m=1}^{M} e^{ikr\cos(\phi_m-\beta)}e^{in(\phi_m-\phi_k)}\delta_m. \tag{15}$$

Recognizing the factor $e^{ikr\cos(\phi_m-\beta)}$ as a plane-wave component with an angle of propagation ϕ_m, we can write that

$$S_{m,k}=-\sum_{n=-N}^{N} i^n\alpha_n\frac{e^{-in\pi/2}}{\pi}e^{in(\phi_m-\phi_k)}\delta_m. \tag{16}$$

This represents the discrete amplitude of plane-wave component ϕ_m caused by the scattering of the incident wave component ϕ_k from the cylinder.

We partition the scattering matrix, $S_{m,k}$, into smaller matrices R^{du}, T^{dd}, R^{ud}, and T^{uu} representing energy incident from above the cylinder and backscattered, downward transmitted energy, etc. It should be noted that the transmission matrices for objects have the form $I+T$ as the transmitted field consists of the scattered field summed with the incident plane wave.

II. NUMERICAL IMPLEMENTATION

In Fig. 2 we showed a sketch of a possible integration contour, C, in the complex plane which could be used for the integral plane-wave representation of a wave field. However, by applying Cauchy's Theorem of complex analysis, it is possible to deform that particular contour into other contours which yield the same integral result. In particular, we choose as our integration contour with respect to ϕ,

$$\phi=t-i\sigma\sin(t);\quad\frac{-\pi}{2}\leq t\leq\frac{\pi}{2}. \tag{17}$$

This contour yields only approximately the correct integral results as it does not account for all the evanescent energy. The contour of Eq. (17) is now discretized with respect to t according to some quadrature scheme; in particular we use the trapezoidal rule. Because we have changed the variable of integration from ϕ to t, the weighting function

$$w(\phi)=\frac{d\phi}{dt}=1-i\sigma\cos(t), \tag{18}$$

must be included in the integrand. The parameter σ controls the offset of the contour from the real-axis; it is the absolute value of the imaginary offsets of the contour at $\phi=\pm\pi/2$. The offset as defined by $-\sigma\sin(t)$ is positive for ϕ having a negative real part and negative for ϕ having a positive real part. The contour passes through $\phi=(0,0)$. For some of the numerical examples, we will also include some additional points along the lines $\phi=\pm\pi/2$ starting at the terminating points of the contour specified in Eq. (17). In these cases, more of the evanescent spectrum is included in the modeling.

The discretization of the integral defines the set of discrete ϕ_j values we use for our operators. The discretization size of ϕ, $\Delta\phi$, determines how far out in x one can compute (see, for example, Ref. 24 for a discussion of this type of issue). In order to construct a line source at a particular depth z_s, we use the plane-wave representation of the Hankel function,[23]

$$\frac{i}{4}H_0^1(k\sqrt{x^2+(z-z_s)^2})=\frac{i}{4\pi}\int_C e^{ik\sin(\phi)x}e^{ik\cos(\phi)|(z-z_s)|}\,d\phi. \tag{19}$$

This representation is then discretized (for z above z_s and for z below z_s) along the computational contour and the resulting amplitudes of the discrete plane-wave components (defined by the set of angles ϕ_j) yields the incident up- and downgoing plane-wave amplitudes.

In many scattering problems, the object scattering and interface scattering matrices may have some special structure. For example, for flat interfaces the interface matrices are diagonal. The plane-wave scattering matrices for a cylinder are structured, as it is only the angle between the incoming and outgoing plane-wave vectors which is important. However, we have numerically implemented our algorithm assuming full matrices and have made no attempt to exploit any particular structure of the matrices involved. In this way the algorithm can handle very general interface/object scattering problems; however, it is, of course, slower than an implementation which exploits the special structure of the matrices for a particular problem. The computational speed also depends upon the required number of discrete wave number points. This factor depends upon the frequency of interest and the maximum desired range of computation.

We consider four basic examples below; a flat waveguide with no scatterer, a wedge-shaped waveguide with no scatterer, a flat waveguide with a cylindrical scatterer and a wedge-shaped waveguide with a cylindrical scatterer. The frequency of interest is 25 Hz and we consider a horizontal window of 8 km. In all examples, the wave-number integrals along the real axis are discretized with 253 points. This number of points was chosen because the resultant angular spacing is very close to $\frac{1}{4}$ the apex angle of the ASA wedge which, as shall be seen, allows us to construct rather simple matrix operators for this case. This same angular spacing was then used for all the examples. For flat waveguide examples, we augment this contour with 24 additional points with varying imaginary parts along each of the vertical lines at $\phi = \pm \pi/2$. The spacing between these points, in terms of their imaginary part, is the same as the spacing Δt used for the discretization of t in Eq. (17).

These additional components are weighted by a taper (a sine function going from one to zero) which goes to zero away from the real axis. This is done in order to minimize any spectral ringing effects. The choice of the integration contour for problems is somewhat *ad hoc* and in general we recomputed problems with different parameters such as offset from real axis, number of points along the vertical axis, etc. until a stable result was achieved.

Using Eq. (6) it is possible to compute the amplitude of the up- and downgoing plane-wave components. In the examples below we will plot the amplitude of the upgoing plane-wave components along the line $z=0$. The location of the line $z=0$ is arbitrary for a problem and may be chosen to correspond to some convenient location; the source depth, an interface, etc. However, the amplitudes of the nonevanescent plane-wave components will not depend upon the location of this line. The field can be computed anywhere in the waveguide by using the discretized version of Eq. (9) above and below the scattering region, with the plane-wave components as given in Eq. (6). When the scatterer is a cylinder we can, in fact, extend the definitions of the upgoing and downgoing plane-wave amplitudes to the horizontal line passing through the center of the cylinder. Alternatively, we can use the effective incident plane waves upon the cylinder as computed by the plane-wave method to generate the coefficients for the Fourier–Bessel representation of the scattered field—this representation is valid in the scattering region and, in fact, in the entire homogeneous waveguide. We will use this approach for the whole waveguide in two-dimensional pressure amplitude computations—we compute the effective incident field in terms of plane waves and scattered field in terms of the resulting Fourier–Bessel series. For the cylinder scattering problem in a wedge we use the Fourier–Bessel representation of the scattered field everywhere in the waveguide. However at the bottom interface we use the plane-wave representation to allow us to easily transmit the field into the bottom half-space.

To compute the scattering matrix from a cylinder we use eleven terms in the Fourier–Bessel series expression of the field scattered from a cylinder. By numerical experimentation we determined that the series had converged sufficiently with this number of terms (for the cylinder in the perfect waveguide example, the upgoing wave components computed using six terms and eleven terms in the Fourier–Bessel series had an average difference of 2.6×10^{-5} dB over an 8-km window) From the NAG library[25] we used a general purpose complex matrix inversion routine and routines for computing sequences of Bessel and Hankel functions (sequences of the form $[J_{\upsilon+n}(x),\ n=1,\ldots,N]$ and $[H^1_{\upsilon+n}(x),\ n=1,\ldots,N]$, for input values of υ, x, and N. It took approximately 8 min of CPU time on a VAX 6000/610 computer in order to compute all the plane-wave coefficients for the cylinder in the wedge example. As mentioned above, it is probably possible to significantly reduce the computation times for these specific examples. The computation of the field in the waveguide, using the plane-wave or Fourier–Bessel coefficients takes additional time.

III. EXAMPLES

A. Flat Pekeris waveguide

As a first example, we consider a waveguide 200 m deep with the parameters of the ASA benchmark wedge;[19] namely in the water column, $c=1500$ m/s, $\rho=1$ kg/m^3 and in the basement $c=1700$ m/s, $\rho=1.5$ kg/m^3, and there is an attenuation $\lambda=0.5$ dB/wavelength. The velocity ratio at the water/basement interface corresponds to a critical angle of propagation in the water of 28.07°. A 25-Hz source is located at a depth of 100 m and there is a receiver at 30 m. We have no scatterer in the waveguide so that the object's transmission matrices are the identity matrix and the object's reflection matrices are zero. The bottom surface matrix is defined with the appropriate plane-wave reflection coefficients for the angles of incidence. We use 253 values of ϕ and set $\sigma=0.15$ in Eq. (8). In Fig. 3(a) we show a plot comparing the pressure amplitude using this method (solid line) and using a discrete/leaky mode code due to Zhang and Tindle[26] (dashed). The curve computed by the plane-wave method is shown for both negative and positive values of x.

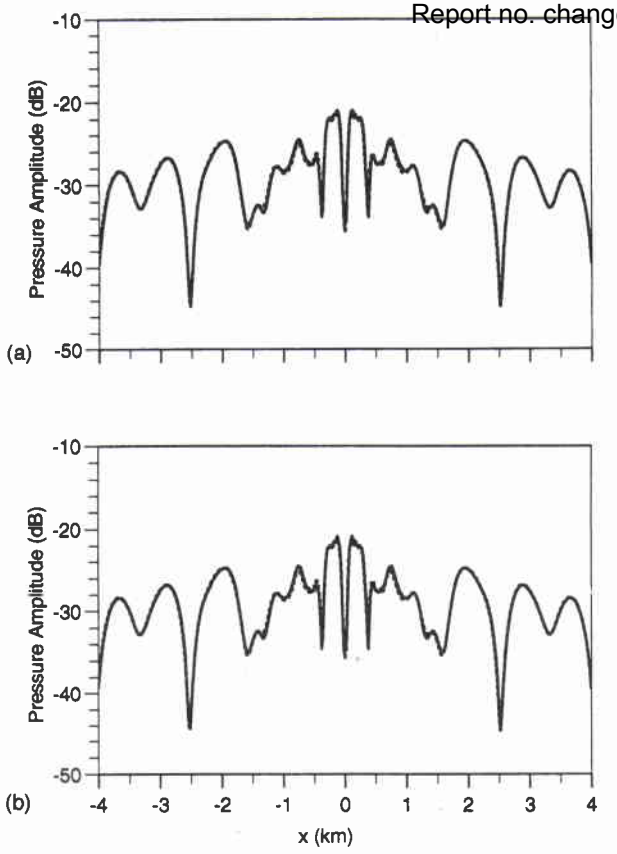

FIG. 3. Pressure amplitude as a function of range for 25-Hz source at 100 m and receiver at 30 m for wave-number method (solid) and modal method (dashed) for flat (ASA) waveguide using (a) $\sigma=0.15$ (b) or $\sigma=0.02$.

As can be seen the two methods are in excellent agreement. In Fig. 3(b) we show the pressure amplitude computed with $\sigma=0.02$ (solid line) and the modal pressure amplitude (dashed). Once again, the agreement is excellent. In Fig. 4 we show the amplitude of the upgoing wave components for the two values of σ (along the $z=0$ line) as a function of the real part of the angle (the imaginary components along the the vertical lines $\phi=\pm\pi/2$ in the complex plane are not shown). The spectrum for $\sigma=0.15$ is significantly smoother than that for $\sigma=0.02$. However, as expected from theory, the computed pressure fields in Fig. 3(a) and (b) are essentially identical. In practice, however, one cannot take arbitrarily small values of σ as it becomes increasingly difficult to accurately represent the wave number integrand. In this and the following examples, negative angles in the spectral plots correspond to plane waves propagating to the left and positive angles corresponds to plane waves propagating to the right. For a flat waveguide, the spectrum will be symmetric about the zero angle.

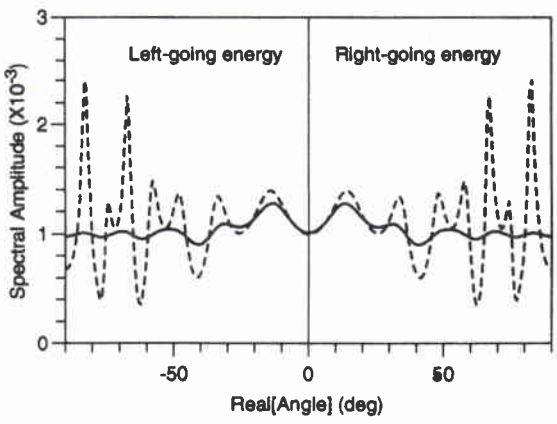

FIG. 4. Spectral amplitudes (upgoing plane waves) along the integration contour for $\sigma=0.15$ (solid line) and $\sigma=0.02$ (dashed line).

B. The ASA wedge

We now consider a waveguide with the same parameters as above but with a sloping bottom of 2.86°. This is one of the ASA benchmark wedges.[19] For the wedge, there are two Cartesian coordinate systems of interest, one which is parallel to the upper interface which we will define as $z=0$ and one parallel to the sloping interface. We relate the plane waves in the two systems by a sequence of matrices. First we define an operator Ω which relates the angles of the plane-wave components from the horizontal coordinate system to the sloping system. This matrix will have a particularly simple form if the angular discretization is a submultiple of the wedge angle. For the ASA benchmark wedge, the wedge angle of 2.86° corresponds approximately to the value $\pi/63$, so that by using an angular stepsize that is an integer submultiple of $\pi/63$ the transformation operator Ω is a simple band matrix; e.g., $\Omega_{i,j}=1$ if $j=i+k$, where k corresponds to the closest number of discrete step sizes corresponding to a shift of $-2.86°$. This procedure is certainly not perfect for this example; this shifting procedure is really only valid along a line of angular values parallel to the real axis. (For example, if a curved contour was used then a point on the contour shifted by 2.86° would no longer lie on the contour and our simple rotation matrix formulation could not be used). We used 253 points along the real axis which corresponds to $k=4$ in the discussion above. In order to describe the interaction of the plane waves with the bottom, the plane-wave components in the horizontal system are first converted to components in the wedge system using Ω. Each component is then advanced in phase corresponding to the normal distance in the wedge system from the origin (source point) to the bottom. This phase advancement is accomplished by using a diagonal matrix. The bottom reflection operator is then applied and the waves are propagated up in the wedge and converted back to the horizontal system (the operator Ω can be used again). These upgoing wave components are reflected downward by the top pressure release surface and there is an iterative sequence of reverberations between the upper and lower surface. These interactions can all be expressed in terms of the upper and lower reflection matrices, Ω, and the phase advancement matrix. The matrix series representing these multiple interactions can then be summed as in Sec. I.

In order to have a smooth integrand it is preferable, as described previously, to deform the integration contour into the complex plane. However, as discussed above, our simple formulation is not strictly valid for a curved contour. As a compromise, we use a value of $\sigma=0.01$ in Eq. (8). We found that the numerical agreement with FEPE[27] became better as the contour came closer to the real axis. However for values

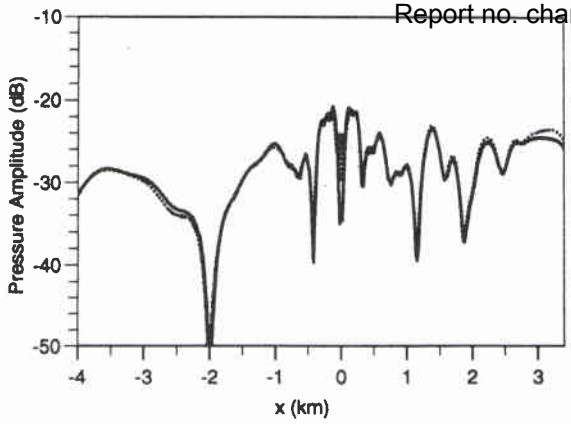

FIG. 5. Up and downslope pressure amplitude for 25-Hz source at 100 m and receiver at 30 m for wave-number method (solid) and FEPE (dashed) for ASA wedge.

of σ less than 0.01 the computed pressure amplitude curve starts to become erratic in appearance. Although we have formally applied the theory of up- and downgoing wave fields, this theory is not always valid for the wedge geometry. For example, upgoing waves with angles of propagation less than 2.86° from the horizontal are downgoing in the coordinate system of the bottom. In this case, it is difficult to cleanly split the plane-wave components into up- and downgoing components. Keeping mind of these theoretical difficulties, we employ the formulation described above.

In Fig. 5 we show the wedge solution (forward and backward energy) as computed with the operator method (solid line) and as computed by FEPE (dashed) where we have removed the $\sqrt{r}$ spreading. One can see that the curve from the operator approach agrees very well with the FEPE curve. In Fig. 6 we show the spectral amplitude of the upgoing plane waves as a function of the real part of the angle of incidence. The features of the positive θ portion of the spectrum seem to be shifted to the left and "stretched" in the negative portion of the spectrum.

This wedge example is an extreme case where the decomposition of the wave field into up- and downgoing plane waves is not exact. However, incorporating the scattering effects of the interface was trivial in this formulation. A similar but more rigorous approach to wedge propagation

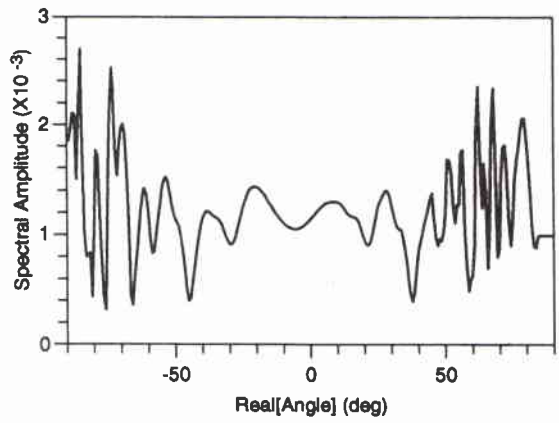

FIG. 6. Spectral amplitudes (upgoing plane waves) for ASA wedge σ=0.02.

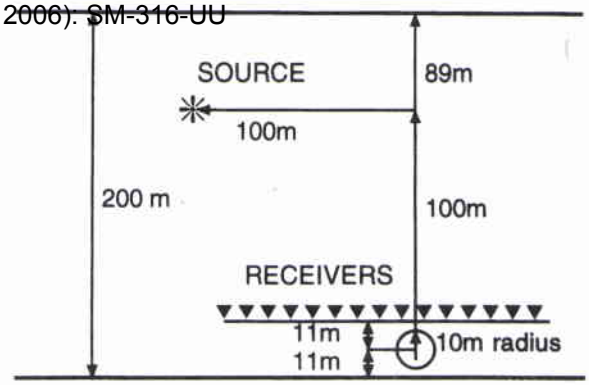

FIG. 7. Geometry of cylinder in waveguide for numerical example 3.

has been described.[28–30] For more general surfaces, the scattering matrix for the surface would have to be found numerically or by employing some approximation such as perturbation theory, Kirchoff approximation, etc.

C. A cylinder in a flat and a wedge-shaped waveguide

In this example we consider a 200-m deep waveguide with two pressure release surfaces. Within the waveguide, an infinite cylinder of radius 10 m (see Fig. 7) is located 11 m above the bottom interface. The boundary condition on the cylinder is also pressure release.

This same problem can also be solved by using a BIEM technique where we use the modal waveguide Green's function[1,2] in order to restrict the integral equation to the surface of the cylinder. We now compute the total pressure field for a source 100 m to the left and above the object. The cylinder's lower edge is taken to be only 1 m above the bottom interface and the line of receivers is taken to be only 1 m above the top of the cylinder (see Fig. 7). Thus this example should be a stringent test on the abilities of the operator method. As can be seen in Fig. 8, the fields as computed by the BIEM and the operator method are in excellent agreement. There is some disagreement close to the

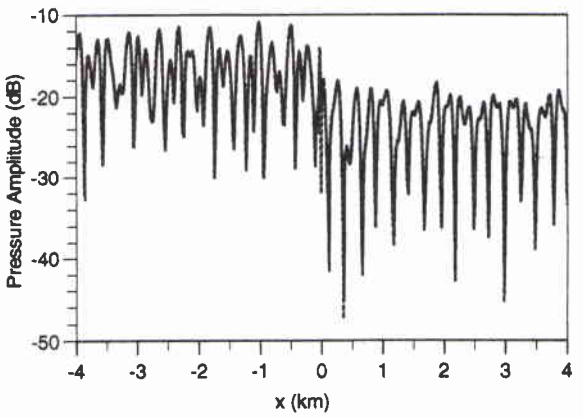

FIG. 8. Pressure amplitude as a function of range (solid—wave number method, dashed—modal BIEM) for a 25-Hz source located 100 m above and to the left of a 10-m radius cylinder with center 11 m above lower pressure release boundary. The receivers are to the left and right of the cylinder at 1 m above the upper limit of the cylinder. The perfect waveguide is 200 m deep.

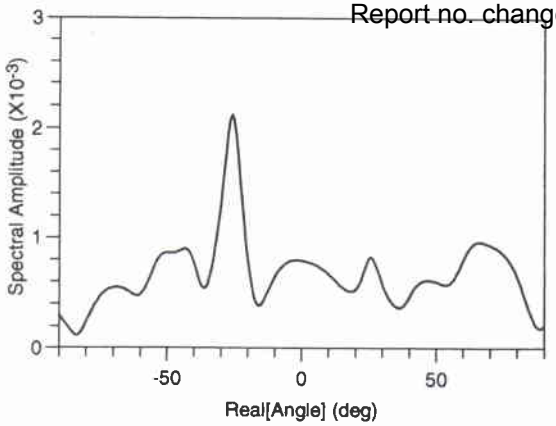

FIG. 9. Spectral amplitudes (upgoing plane waves) for perfect waveguide with cylinder $\sigma=0.15$.

origin—the agreement in this region becomes better if we include more evanescent components in the plane-wave decomposition method, corresponding to more points along the lines $\phi=\pm\pi/2$. However, for the longer ranges of Fig. 8 we wished to concentrate our wave-number coverage along the real axis and used only 24 points along each of the lines $\phi=\pm\pi/2$. Alternatively, if we compute the scattered field from the computed "effective" incident plane-wave field using the Fourier–Bessel series we get better agreement in this very near-field region. This is probably due to the fact that the Hankel functions, in their plane-wave decomposition, contain much of the necessary evanescent components.

In Fig. 9 we show the spectrum of the upgoing plane-wave components. The spectrum has a significant component at a negative angle (measured off the vertical) of about 25°. This angle corresponds to the last mode (mode 6) before cutoff propagating to the left in the waveguide.

In Fig. 10(a) we show a two-dimensional gray-scale plot of the wave field in a 200-m square about the cylinder. As discussed above, there are a number of ways to generate this field once the plane-wave coefficients above and below the scattering object are known. We use the computed downgoing (upgoing) plane-wave coefficients above (below) the cylinder to specify the "incident" field and generate the "scattered" field using Eq. (11). This is not the usual definition of the scattered field as our "incident" plane-wave coefficients also include the effect of the scattering object. To isolate the effect of the cylinder on the wave field we compute the wave field when there is no cylinder present and subtract this field from the field with the cylinder present. The resulting difference is plotted in Fig. 10(b).

It is very easy to now repeat the computations for a penetrable basement (we again use the geoacaoustic parameters of the ASA wedge) by simply defining the reflection coefficients as a function of the angle of incidence. In Fig. 11(a) and (b) we show the total and scattered fields for a 200-m square about the cylinder.

Finally, we consider the ASA wedge and place the pressure-release cylinder in this waveguide at a depth of 150 m. The cylinder transmission and reflection matrices are combined with the rotation matrix Ω described in the previous section in order to compute the resultant pressure field.

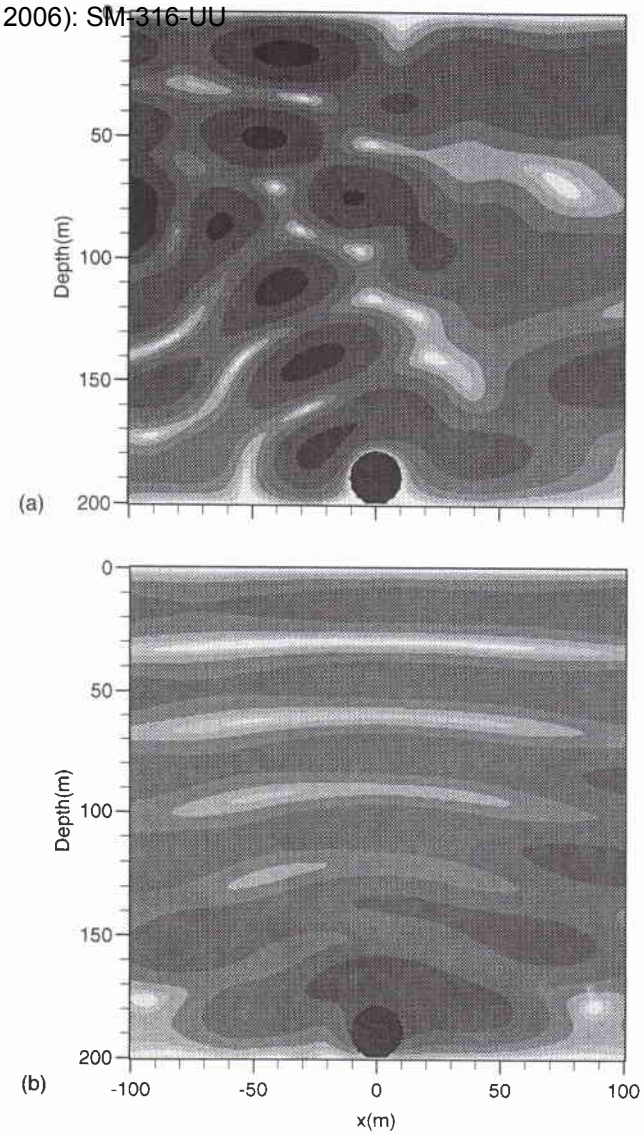

FIG. 10. (a) Total wave field. (b) Wave field due to presence of cylinder for pressure release bottom. Gray-scale levels of 5-dB increment from below −40 dB (light) to above −15 dB (dark).

In Fig. 12(a) and (b) we show two-dimensional plots of the total and scattered fields from the cylinder in the wedge. In this example, however, the cylinder is located at a depth of 150 m in the waveguide where the basement is at 200 m. The source is 50 m above and 100 m to the left of the cylinder center. We compute this field in the same manner as for the flat waveguide. In order to compute the field in the basement we used the downgoing plane-wave representation; each component is converted to the sloping coordinate system, multiplied by the appropriate transmission coefficient, and propagated in the basement. In Fig. 12(b) there are slight high-frequency oscillations in the computed scattered field in the left part of the grid. These may be partially due to small artifacts from the approximations of the method (in the wedge case) itself and the numerical discretizations used. It is important to note that we can easily use the above theory for a more complicated cylindrical structure in a waveguide. The solution of a more general cylinder scattering problem is first determined in terms of its Hankel function expansion

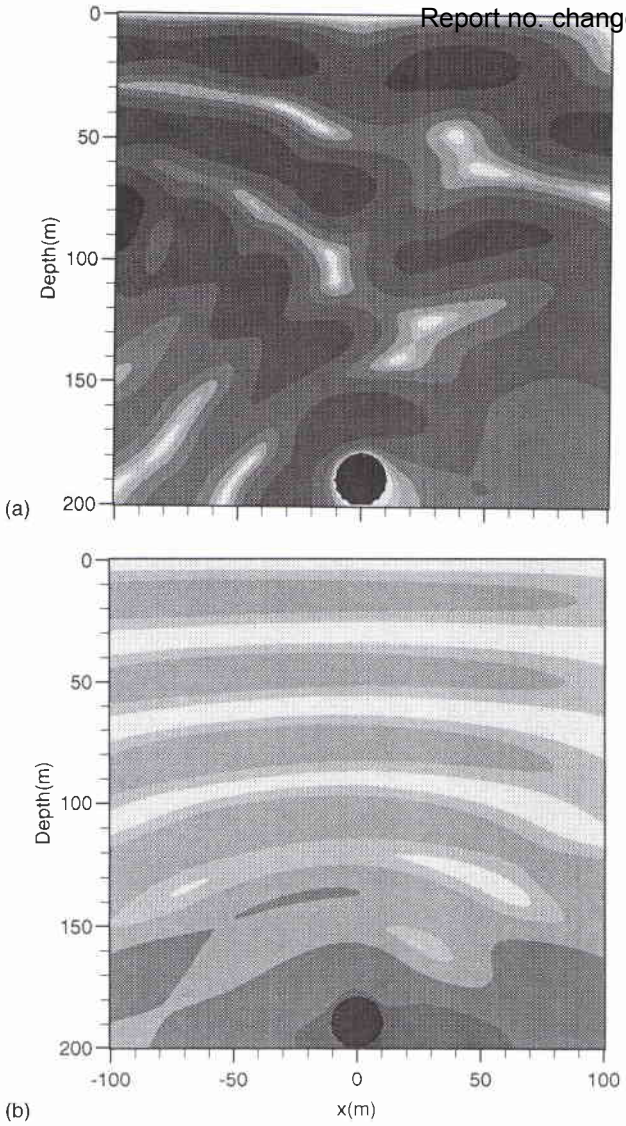

FIG. 11. (a) Total wave field. (b) Wave field due to presence of cylinder for penetrable bottom. Gray-scale levels of 5-dB increment from below −40 dB (light) to above −15 dB (dark).

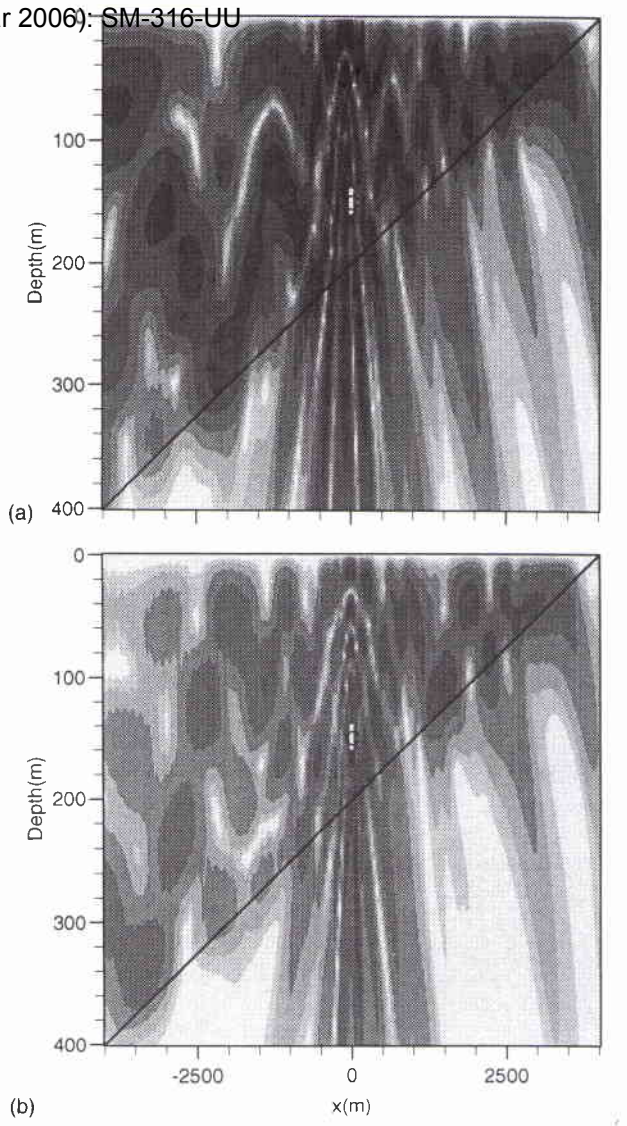

FIG. 12. (a) Total wave field. (b) Wave field due to presence of cylinder in a wedge. Gray-scale levels of 5-dB increment from below −50 dB (light) to above −25 dB (dark). Cylinder is indicated by lowest gray level and a "C."

which then defines the plane-wave scattering matrix through Eqs. (14)–(16). The rest of the computation proceeds as above.

IV. SUMMARY AND DISCUSSION OF RESULTS

A straightforward method of including the scattering matrices from objects and/or interfaces in waveguide modelling, following the work of Kennett and others[14–16] for interface scattering, has been presented. The methodology of this paper is not dependent on how the individual scattering matrices are computed. The overall accuracy of the final result is, of course, very dependent on the accuracy of the individual scattering matrices. The complete waveguide solution is computed combining the object and interface scattering matrices in a manner analogous to standard modeling in a stratified medium. We chose simple examples but the inclusion of complicated stratification, elastic parameters, etc. is straightforward.

We considered the object within a homogeneous layer; however, a depth-varying sound speed can be easily handled as long as the layer about the object can be considered to be homogeneous. If this is not a valid assumption, then the free-space scattering problem to be solved for the object must be solved with a surrounding depth-dependent sound speed.

[1] T. W. Dawson and J. A. Fawcett, "A boundary integral equation method for acoustic scattering in a waveguide with nonplanar surfaces," J. Acoust. Soc. Am. **87**, 1110–1125 (1990).
[2] P. Gerstoft and H. Schmidt, "A boundary element approach to seismo-acoustic facet reverberation," J. Acoust. Soc. Am. **89**, 1629–1642 (1991).
[3] A. Bostrom, "Transmission and reflection of acoustic waves by an obstacle in a waveguide," Wave Motion **2**, 167–184 (1980).
[4] G. S. Sammelman and Roger H. Hackman, "Acoustic scattering in a homogeneous waveguide," J. Acoust. Soc. Am. **82**, 325–336 (1987).
[5] R. Lim, "Scattering by an obstacle in a plane-stratified poroelastic medium: Application to an obstacle in ocean sediments," J. Acoust. Soc. Am. **95**, 1223–1244 (1994).
[6] M. Dougherty and R. Stephen, "Geoacoustic scattering from seafloor features in the ROSE area," J. Acoust. Soc. Am. **82**, 239–256 (1987).
[7] J. E. Murphy and S. A. Chin-Bing, "A seismo-acoustic finite element

model for underwater acoustic propagation," in *Shear Waves in Marine Sediments*, edited by J. M. Hovem, M. D. Richardson, and R. D. Stoll (Kluwer Academic, Dordrecht, The Netherlands, 1991), pp. 463–470.
[8] R. B. Evans, "A coupled mode solution for acoustic propagation in a waveguide with stepwise depth variations of a penetrable bottom," J. Acoust. Soc. Am. **74**, 188–195 (1993).
[9] D. P. Knobles, "Solutions of coupled-mode equations with a large dimension in underwater acoustics," J. Acoust. Soc. Am. **96**, 1741–1747 (1994).
[10] M. D. Collins and M. F. Werby, "A parabolic equation model for scattering in the ocean," J. Acoust. Soc. Am. **85**, 1895–1902 (1989).
[11] F. Ingenito, "Scattering from an object in a stratified medium," J. Acoust. Soc. Am. **82**, 2051–2059 (1987).
[12] G. V. Norton and M. F. Werby, "A numerical technique to describe acoustical scattering and propagation from an object in a waveguide," J. Appl. Phys. **70**, 4101–4112 (1991).
[13] M. D. Collins and R. B. Evans, "A two-way parabolic equation for acoustic backscattering in the ocean," J. Acoust. Soc. Am. **91**, 1357–1368 (1992).
[14] B. L. N. Kennett, "Reflection operator methods for elastic waves I—Irregular interfaces and regions," Wave Motion **6**, 407–418 (1984).
[15] K. Kohketsu, "2D reflectivity method and synthetic seismograms for irregularly layered structures—I SH-wave generation," Geophys. J. R. Astron. Soc. **89**, 821–838 (1987).
[16] B. L. N. Kennett, K. Koketsu, and A. J. Haines, "Propagation invariants, reflection and transmission in anisotropic, laterally varying media," Geophys. J. Int. **103**, 95–101 (1990).
[17] L. Neil Frazer and John J. McCoy, "An acoustic reflectivity method for laterally varying media," in *OCEAN SEISMO-ACOUSTICS Low-Frequency Underwater Acoustics*, edited by T. Akal and J. Berkson, NATO Conference Series (Plenum, New York, 1986), pp. 47–55.
[18] G. T. Schuster and L. C. Smith, "Modeling scatterers embedded in a plane-layered media by a hybrid Haskell–Thomson and boundary integral equation method," J. Acoust. Soc. Am. **78**, 1387–1394 (1985).
[19] F. B. Jensen and C. M. Ferla, "Numerical solutions of range-dependent benchmark problems in ocean acoustics," J. Acoust. Soc. Am. **87**, 1499–1510 (1990).
[20] D. K. Dacol, "The Kirchoff approximation for scattering from a rough fluid-elastic solid interface," J. Acoust. Soc. Am. **88**, 978–983 (1990).
[21] T. Yang and S. Broschat, "Acoustic scattering from a fluid-elastic solid interface using the small slope approximation," J. Acoust. Soc. Am. **96**, 1796–1804 (1994).
[22] B. L. N. Kennett, *Seismic Wave Propagation in Stratified Media* (Cambridge U.P., Cambridge, 1983).
[23] J. A. Stratton, *Electromagnetic Theory* (McGraw-Hill, New York, 1941).
[24] H. Schmidt, "SAFARI Seismo-Acoustic Fast Field Algorithm for Range-Independent environments—User's Guide," SACLANTCEN Report SR-113, SACLANT Undersea Research Centre, September 1988.
[25] NAG Fortran Library, Mark 15, Numerical Algorithms Group, 1991.
[26] Z. Y. Zhang and C. T. Tindle, "Complex effective depth of the ocean bottom," J. Acoust. Soc. Am. **93**, 205–213 (1993).
[27] M. D. Collins, "FEPE User's Guide," NORDA TN-365, Naval Ocean Research and Development Activity, Stennis Space Center, MS (1988).
[28] A. P. Ansbro and J. M. Arnold, "Numerically efficient evaluation of intrinsic modes in wedge-shaped waveguides," J. Acoust. Soc. Am. **89**, 1623–1642 (1991).
[29] J. M. Arnold and L. B. Felsen, "Intrinsic modes in a nonseparable ocean waveguide," J. Acoust. Soc. Am. **76**, 850–860 (1984).
[30] J. M. Arnold and L. B. Felsen, "Coupled mode theory of intrinsic modes in a wedge," J. Acoust. Soc. Am. **79**, 31–40 (1986).

Report no. changed (Mar 2006): SM-316-UU

Document Data Sheet

NATO UNCLASSIFIED

Security Classification		Project No.
UNCLASSIFIED		033-3
Document Serial No.	**Date of Issue**	**Total Pages**
SM-316	November 1996	16 pp.

Author(s)

J.A. Fawcett

Title

A plane-wave decomposition method for modeling scattering from objects and bathymetry in a waveguide

Abstract

In this paper a straightforward plane-wave decomposition method which can be used for solving object and/or interface scattering problems in a waveguide is described. The method utilizes the free-space scattering matrices in conjunction with the medium's interface and layer matrices in order to solve the waveguide scattering problem.

Keywords

Issuing Organization

North Atlantic Treaty Organization
SACLANT Undersea Research Centre
Viale San Bartolomeo 400, 19138 La Spezia, Italy

[From N. America: SACLANTCEN CMR-426 (New York) APO AE 09613]

Tel: +39 (0)187 540 111
Fax:+39 (0)187 524 600

E-mail: library@saclantc.nato.int

NATO UNCLASSIFIED

Initial Distribution for SM-316

SCNR for SACLANTCEN		*National Liaison Officers*	
SCNR Belgium	1	NLO Canada	1
SCNR Canada	1	NLO Denmark	1
SCNR Denmark	1	NLO Germany	1
SCNR Germany	1	NLO Italy	2
SCNR Greece	2	NLO Netherlands	1
SCNR Italy	1	NLO UK	3
SCNR Netherlands	1	NLO US	4
SCNR Norway	1		
SCNR Portugal	1		
SCNR Spain	1		
SCNR Turkey	1		
SCNR UK	1		
SCNR US	2		
French Delegate	1		
SECGEN Rep. SCNR	1	Total external distribution	34
NAMILCOM Rep. SCNR	1	SACLANTCEN Library	26
SACLANT	3	Total number of copies	60